

# Structural and Optical Properties of ( $\text{Li}_x\text{Ni}_{2-x}\text{O}_2$ ) Thin Films Deposited by Pulsed Laser Deposited (PLD) Technique at Different Doping Ratio

Khalid. H. Razeg<sup>1</sup>, Muthafar. F. AL-Hilli<sup>2</sup>, Abed. A. Khalefa<sup>1\*</sup>, Kadhim A. Aadim<sup>2</sup>

<sup>1</sup>Department of Physics, University of Tikrit, College of Education

<sup>2</sup>Department of Physics, University of Baghdad, College of Sciences

\*Corresponding author: abedkhalefa65@gmail.com

**Abstract** This paper study ( $\text{Li}_x\text{Ni}_{2-x}\text{O}_2$ ) thin films with different value of  $x$  ( $x = 0.0, 0.15, 0.25, 0.35$  and  $0.45$ ) prepared by pulse laser deposition technique (PLD) on a glass bases and annealed to ( $350^\circ\text{C}$ ). Using X-ray diffraction (XRD) and atomic force microscopy (AFM) to study the properties of synthetic and show that the (NiO) film has face centre cubic structure (fcc), while the ( $\text{Li}_x\text{Ni}_{2-x}\text{O}_2$ ) films of the ratio (0.15 to 0.45) has a hexagonal installation and grain size increase with the doping. Optical properties studied within the specified range of wavelengths (300-1100nm), it's found that the energy gap and transmittance decrease while absorbance and extinction coefficient increase with the doping.

**Keywords:** ( $\text{Li}_x\text{Ni}_{2-x}\text{O}_2$ ) thin film, (PLD) Technique, Optical Properties

**Cite This Article:** Khalid. H. Razeg, Muthafar. F. AL-Hilli, Abed. A. Khalefa, and Kadhim A. Aadim, "Structural and Optical Properties of ( $\text{Li}_x\text{Ni}_{2-x}\text{O}_2$ ) Thin Films Deposited by Pulsed Laser Deposited (PLD) Technique at Different Doping Ratio." *International Journal of Physics*, vol. 5, no. 2 (2017): 46-52. doi: 10.12691/ijp-5-2-3.

## 1. Introduction

A nickel oxide (NiO) in the form of crystalline powder dark green color tends to darkening has mass density ( $6.67\text{g} / \text{cm}^3$ ), and Molecular weights ( $842.87\text{g} / \text{mole}$ ) [1]. The thin film of nickel oxide (NiO) has face center cubic structure (fcc), (P-type) and broad energy band gap lies in the range ( $3.6 - 4\text{eV}$ ). NiO films are manufactured or installed in various physical and chemical deposition techniques, which include: spraying pyrolysis [2], colloidal solution (sol-gel) [3], RF- sputtering [4], Negative way spraying (D.C sputtering) [5], and pulsed laser deposition (PLD) [6,7]. ( $\text{LiNiO}_2$ ) is similar to ( $\text{LiCoO}_2$ ) where the films appeared in hexagonal structure [8] The compounds (Li-Ni-O) typically contain oxygen atom for each metal atom and is based on the compact layers (close -packed) of oxygen atoms. ( $\text{LiNiO}_2$ ) used in poles cathode of the lithium batteries and lithium-ion due to its ease of production and processing and has a relatively long life cycle and the percentage of low self-emptying, the pole cathode in overlapped ( $\text{LiNiO}_2$ ) has a high electrical capacity and effort electrician is lower than it is in compound ( $\text{LiCoO}_2$ ). nickel compounds are often cheaper than oxides containing cobalt.

## 2. Experimental Survey

Nickel oxide powder (NiO) laboratory purity (99.99%),

as well as lithium carbonate powder ( $\text{Li}_2\text{CO}_3$ ) laboratory itself purity (99.99%) were brought and mixing in a mixture according to the value of  $x$  in the compound  $\text{Li}_x\text{Ni}_{2-x}\text{O}_2$  ( $x = 0.00, 0.15, 0.25, 0.35, 0.45$ ) Was calculated as weight percentages of powders using a digital electronic balance sensor type (Mettler. A.K-160) sensitivity ( $10^{-4}\text{ gm}$ ). The grinding powders weighted by mortar casserole (size: 3) for half an hour, and then was put powders milled plastic canisters inside three ceramic balls diameter (0.50 cm) and then put each package inside the mixing English origin type device (spex Mixer) for ten minutes, then pressed the powders blended with compressive strength ( $10^7\text{N} / \text{m}^2$ ) in a special mold (steel stainless) in diameter (1.2 cm) and thickness (0.3 cm) for a period of (3sec) by piston hydraulic American origin factory by a company (across international). Sintering discs in the electric furnace to ( $950^\circ\text{C}$ ) in the presence of oxygen gas ( $\text{O}_2$ ) for two hours. Glass slides of geometric dimensions ( $75 \times 25 \times 1.2\text{ mm}$ ) (Chinese-made type AFCO) for the deposition of thin films of the compound after washed it with distilled water and ethanol with a purity (96%).  $\text{Li}_x\text{Ni}_{2-x}\text{O}_2$  films were deposited by PLD within a vacuum chamber in the system of pulsed laser surgery type (Nd-YAG pulse laser) under pressure ( $10^{-3}\text{ Torr}$ ). The deposition process and the growth of thin films in a way (PLD) includes three basic steps are: 1. interaction of pulsed laser package with the goal, which is a ceramic disk. 2. The formation and expansion of the plasma inside the deposition chamber toward the glass slide that is by sedimentation caused by lasers. 3. Deposition of the film on the glass slide at room

temperature at low discharge pressure of the occasion laser energy to precipitate the membranes (800m.J) and frequency (6Hz) which manufactures laser fallen with the target surface angle (45°), and prove the glass slide in front of the goal and distance (1-3) cm, and the distance between the target and a starting point lasers (15 cm).

## 2.1. Structure and Composition Measurements

### a-X-Ray Diffraction

Crystal structure of ( $\text{Li}_x\text{Ni}_{2-x}\text{O}_2$ ) films prepared on glass by PLD have been studied at 350°C using X-ray diffraction device model (Philips PW 1840). The device record the intensity as a function of Bragg's angle, Grain size ( $G.s$ ) which plays an important role in materials characteristics can be estimated easily from the spectrum X-rays by Shearer formula applied in account granular size.

$$G.S = \frac{0.94\lambda}{\beta \cos\theta} \quad (1)$$

Where:  $K=0.94$ ,  $\lambda$  =wave length,  $\beta$  = (FWHM),  $\theta$  = Bragg's angle.

### b-Atomic Force Microscop (AFM)

In this study, the use of an atomic force microscope type ((Scanning probe microscope type AA3000 equipped from (Angstrom Advanced Company), it is characterized by the ability of the high amount of analysis (0.1 - 1.0nm), high zoom power and the possibility of runs under normal atmospheric pressure without the need to unload high as it is in electronic microscopes. this machine gives analytical images of two-dimensional (2 D) and three-dimensional (3 D) to the surfaces of ( $\text{Li}_x\text{Ni}_{2-x}\text{O}_2$ ) films. Its provide us some calculations on the form of granules size, rate of surface roughness and root mean square by computer program prepared from manufacturer.

## 2.2. Optical Properties Measurement

Optical measurements fulfilled for ( $\text{Li}_x\text{Ni}_{2-x}\text{O}_2$ ) films using a spectroscopy device type (UV / Visible SP- 8001

spectrophotometer)) and the extent of spectral (300 - 1100nm). the reset device put glass slide is not precipitator it, then the slide precipitator it membrane placed to be registered to read absorbing spectrum of membrane after subtracting read glass absorption spectrum. All the readings recorded at room temperature. The optical measurements is the absorbance measurement (A) and transmittance (T). using a special software program we get the value of the absorption coefficient, energy band gap and create graphs of relations between the values of those calculated as a function of the incident photon energy and the wavelength.

## 3. Result and Discussion

### 3.1. Structural Properties

#### a-X-ray diffraction:

Figure 1 shows the curves of X-ray diffraction of the film of pure nickel oxide and doping with lithium Oxide in various value of x (x= 0.15, 0.25, 0.35, 0.45) deposited on glass and annealed to (350°C). The curves of thin films show a polycrystalline structure where a multiple peaks appeared in all samples. The curve of pure sample showed that NiO has face center cubic structure (fcc), where three peaks appeared at ( $2\theta = 37.4582, 43.5452$  and  $63.2100^\circ$ ), which date back crystalline levels (111), (200) and (220) and the corresponding standard values. After doping the peaks belonging to the oxide nickel (NiO) disappeared and appeared a new peak for ( $\text{LiNiO}_2$ ) at ( $2\theta = 36.6823, 44.4060$  and  $48.915^\circ$ ), which date back crystalline levels (101), (104) and (015), which shows hexagonal structure as a result of involving the lithium ions in the crystal cube system assortment of nickel oxide this is consistent with [11]. It can be seen that the intensity of the peaks increases with the proportion of doping indicating increased crystallization rate and the width of peaks decrease indicating increased particle size. It can be noticed from Table 1 that the grain size increase with the increasing of doping As well as it can be seen a few shift in a site of peaks as a result of increased doping that led to the existence of deformation in the lattice.

Table 1. Shows the peaks and its Bragg's angle, interplanar distance, and full width half at maximum for ( $\text{Li}_x\text{Ni}_{2-x}\text{O}_2$ ) thin films with various values of x at 350°C

x	$2\theta$ (Deg.)	FWHM (Deg.)	$d_{hkl}$ Exp.(Å)	G.S (nm)	$d_{hkl}$ Std.(Å)	hkl	Phase	card No.
0	37.4582	0.7358	2.3990	11.4	2.4120	(111)	NiO	47-1049
	43.5452	0.8696	2.0767	9.8	2.0885	(200)	NiO	47-1049
	63.2100	0.8530	1.4699	10.9	1.4773	(220)	NiO	47-1049
0.15	36.6823	0.7120	2.4479	11.8	2.4481	(101)	$\text{LiNiO}_2$	09-0063
	44.4060	0.7050	2.0384	12.2	2.0384	(104)	$\text{LiNiO}_2$	09-0063
	48.9150	0.7230	1.8605	12.1	1.8605	(015)	$\text{LiNiO}_2$	09-0063
0.25	36.6930	0.6408	2.4472	13.1	2.4481	(101)	$\text{LiNiO}_2$	09-0063
	44.4190	0.6345	2.0379	13.5	2.0384	(104)	$\text{LiNiO}_2$	09-0063
	48.9280	0.6507	1.8601	13.4	1.8605	(015)	$\text{LiNiO}_2$	09-0063
0.35	36.7060	0.5767	2.4464	14.5	2.4481	(101)	$\text{LiNiO}_2$	09-0063
	44.4320	0.5711	2.0373	15.0	2.0384	(104)	$\text{LiNiO}_2$	09-0063
	48.9410	0.5856	1.8596	14.9	1.8605	(015)	$\text{LiNiO}_2$	09-0063
0.45	36.7190	0.5190	2.4456	16.1	2.4481	(101)	$\text{LiNiO}_2$	09-0063
	44.4450	0.5139	2.0367	16.7	2.0384	(104)	$\text{LiNiO}_2$	09-0063
	48.9540	0.5271	1.8592	16.6	1.8605	(015)	$\text{LiNiO}_2$	09-0063

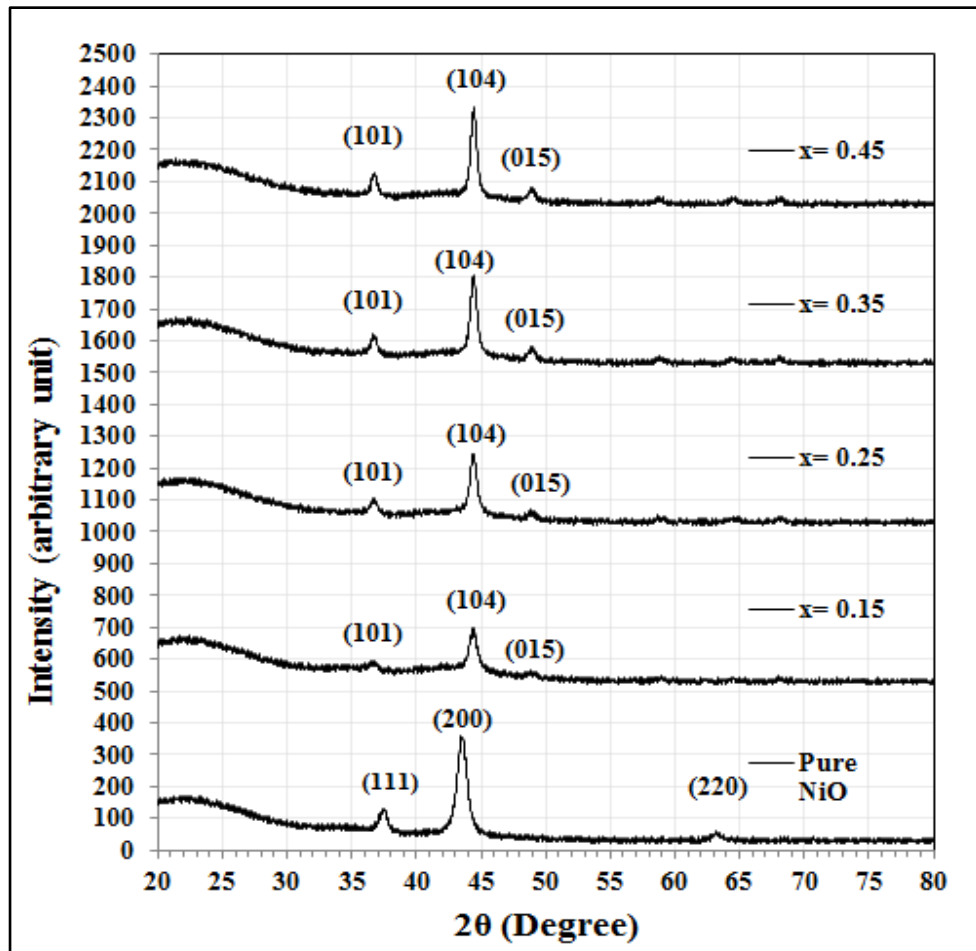


Figure 1. X-ray diffraction for  $(\text{Li}_x\text{Ni}_{2-x}\text{O}_2)$  thin films with various value of  $x$  at  $350^\circ\text{C}$

### b-Atomic Force Microscopy Measurements (AFM)

Figure 2 shows the images of the microscope (AFM) two-dimensional (2-D) and three dimensions (3-D) for measuring areas and analytical capabilities of different topography of the surface of the thin films prepared from the compound  $(\text{Li}_x\text{Ni}_{2-x}\text{O}_2)$ , AFM tests have shown an increase in particle size and a decrease in the values of the rate roughness and the average root mean square of the prepared films as in Table 2. Grain size of films growing with doping up to reach (95.67 nm) at the ratio ( $x = 0.45$ ) and a corresponding decrease in the surface roughness and the value of the average root mean square of the films to (0.615 nm) and (0.820 nm) respectively. Increase granular size and a decrease of both surface roughness rate and the value of the average square root of  $(\text{Li}_x\text{Ni}_{2-x}\text{O}_2)$  films can be explained that doping resulted in uniformity High-crystalline good homogeneity and superficial particles composed of film material and this is in line with [12].

### 3.2. Optical Measurements

It is included the study of optical properties of nickel oxide (NiO) film and  $(\text{Li}_x\text{Ni}_{2-x}\text{O}_2)$  films prepared in a manner (PLD) and annealed at ( $350^\circ\text{C}$ ). The transmittance, absorbance, absorption coefficient, energy band gap and Extinction Coefficient have been studied within the specified range of wavelengths (300-1100nm).

#### a-Transmission(T)

The transmittance measurements within the range

(300-1100nm) of wavelengths for all films prepared from oxide nickel (NiO) and  $(\text{Li}_x\text{Ni}_{2-x}\text{O}_2)$  depending on the value of  $x$  value prepared at annealed temperature ( $350^\circ\text{C}$ ) as shown in Figure 3. NiO films show high transparency in the visible and ultraviolet region amounting permeability to about (85.28%), and the difference in the permeability values may be due to doping process where any changes did not appear in the general shape of the permeability curve, but alloy addition of lithium oxide ( $\text{Li}_2\text{O}$ ) reduces the value of optical permeability. permeability curve for all samples shows similar visually behavior where a sudden and clear increase when the wavelength (370nm). The results showed that the permeability gradually increases with the wavelength for all the films of nickel oxide and this is consistent with [13] and the  $(\text{Li}_x\text{Ni}_{2-x}\text{O}_2)$  films be less as possible for all the films in the UV region in the range of wavelengths (333-352nm) and then permeability starts increase with increasing of wavelength in the area of the visible spectrum (400 - 700 nm), these results are consistent with [14,15]. It was noticed that the permeability decreases with increasing of the value of  $x$  in the compound  $(\text{Li}_2\text{Ni}_{2-x}\text{O}_2)$  as in the Table 3 because the increased concentration of lithium ions in the cationic compound  $(\text{Li}_x\text{Ni}_{2-x}\text{O}_2)$  leads to an increase in the particle size in the crystal structure in the lattice of compound and facilitates the spread of lithium ions in the blanks and all this leads to reducing the permeability of films prepared up doping ratios this is consistent with. [16]



Table 2. AFM measurement for  $(Li_xNi_{2-x}O_2)$  thin films with various values of x at 350°C

sample	T	x	Average diameter (nm)	Average roughness (nm)	r.m.s(nm)	Peak –Peak (nm)
$(Li_xNi_{2-x}O_2)$ (Thin film)	350°C	0	80.12	1.83	2.14	9.54
		0.15	81.62	1.38	1.63	5.80
		0.25	87.31	0.923	1.08	3.91
		0.35	89.31	0.802	1.01	6.39
		0.45	95.67	0.615	0.820	5.30

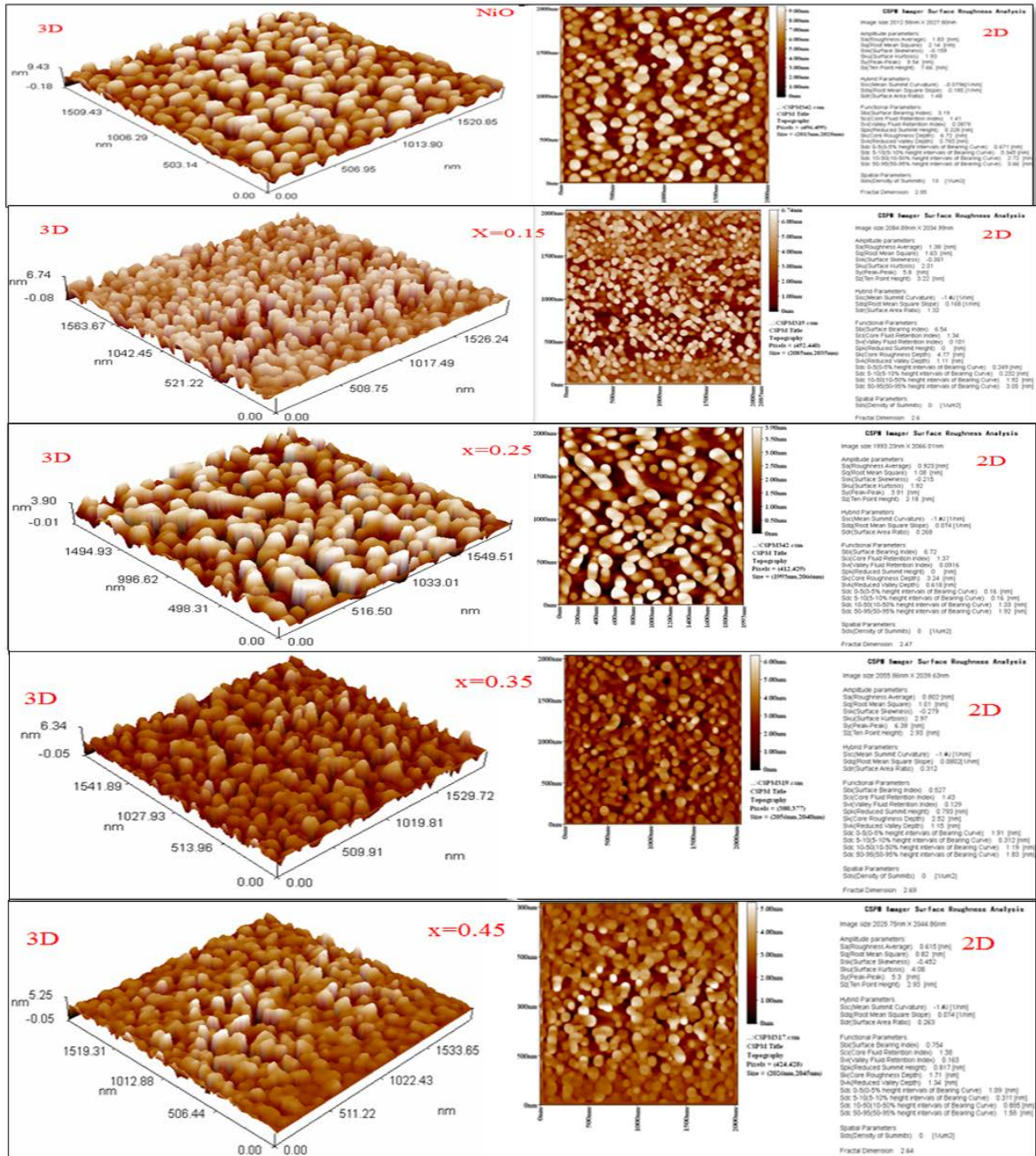


Figure 2. 2-D and 3-D image for  $(Li_xNi_{2-x}O_2)$  thin films with various values of x at 350°C

Table 3. Optical properties for  $(Li_xNi_{2-x}O_2)$  thin films with various values of x at 350°C

T	x	T%	$\alpha$ (cm <sup>-1</sup> )	K <sub>0</sub>	Eg (eV)
350°C	0	85.28	7959	0.04	3.90
	0.15	78.09	12365	0.06	3.56
	0.25	49.20	35466	0.17	3.46
	0.35	49.10	35561	0.17	3.34
	0.45	44.05	40997	0.20	3.32

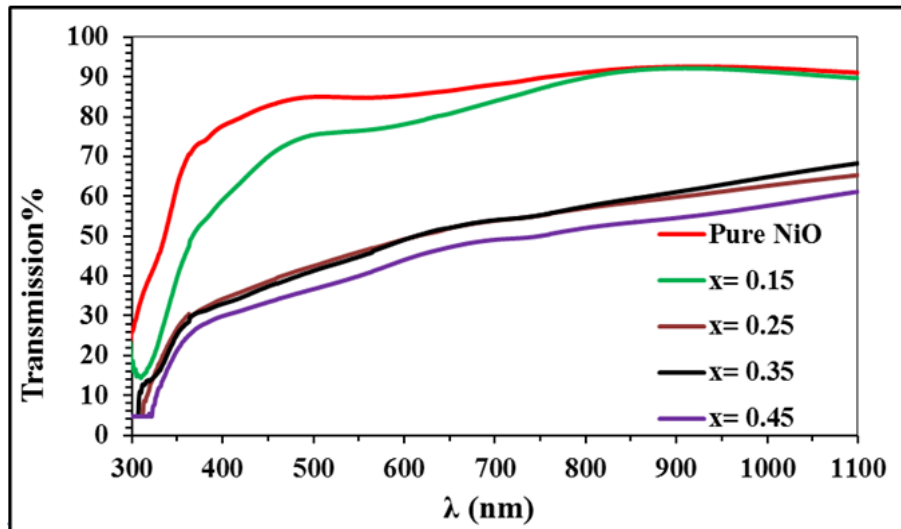


Figure 3. Transmittance for  $(\text{Li}_x\text{Ni}_{2-x}\text{O}_2)$  thin films with various values of  $x$  at  $350^\circ\text{C}$

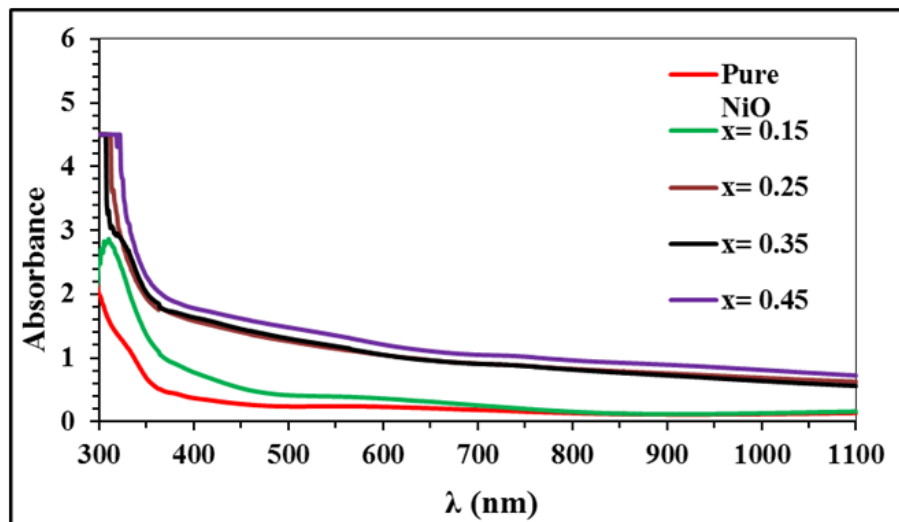


Figure 4. Absorbance for  $(\text{Li}_x\text{Ni}_{2-x}\text{O}_2)$  thin films with various values of  $x$  at  $350^\circ\text{C}$

#### b- Absorbance (A)

Figure 4 shows the absorbance measurements of films prepared from the compound  $(\text{Li}_x\text{Ni}_{2-x}\text{O}_2)$  and annealed to  $(350^\circ\text{C})$ . It was painted graphic relationship of absorbency as a function of wavelength as in Experimental results show that the absorbance gradually decreases with increasing wavelength for all films, and this shows that the energy of photons falling on the thin-film were not enough to excite electrons and transfer of valence band to conduction band, and this means that the photons falling energy is less than the value of the energy gap for all films prepared. We note that the absorbance increases with the increasing value of  $x$  in the compound  $(\text{Li}_x\text{Ni}_{2-x}\text{O}_2)$  can be attributed to increase the absorbance values increase doping and add certain proportions of lithium oxide ( $\text{Li}_2\text{O}$ ) to membranes. The doping compound led to the creation of new levels within the energy gap near the conduction band which caused increase the likelihood absorb photons with low-lying energy, this is consistent with the results of [17]. Absorbance decreases with the increasing of wavelength. Since the absorbance of all films have the greatest value at short wavelengths and then begin to decline with increasing wavelength to reach the lowest

values in the visible spectrum region, where it can be attributed to the photon incident cannot irritate the electron and removed from the valence band to conduction band because the incident photon energy is less than the value of the energy gap of the semiconductor therefore absorbance decrease with increasing wavelength this is consistent with the study. [18]

#### c-Absorption coefficient ( $\alpha$ )

Figure 5 show the graphical relationship between the absorption coefficient and wavelength for all films prepared to  $350^\circ\text{C}$ , the results showed that the absorption coefficient gradually decreases with increasing wavelength for all doping ratios, also showing that the absorption coefficient values of prepared films were ( $\alpha > 10^4\text{cm}^{-1}$ ) which indicate that the films are owned direct energy gap. It is found from chart that the greatest value of the absorption coefficient are at wavelengths corresponding to the UV region then the value start decrease in visual areas and infrared regions of the electromagnetic spectrum. The absorption coefficient increases with the value of  $x$ , which means increasing the proportion of doping lithium oxide in the  $(\text{Li}_2\text{Ni}_{2-x}\text{O}_2)$

films as in Table 3 due to increase the absorbance. the absorbance increases with photon energy and it is obvious that the absorption coefficient is proportional

increases with photon energy because the absorption coefficient depends on the absorbance This is consistent with the study. [17]

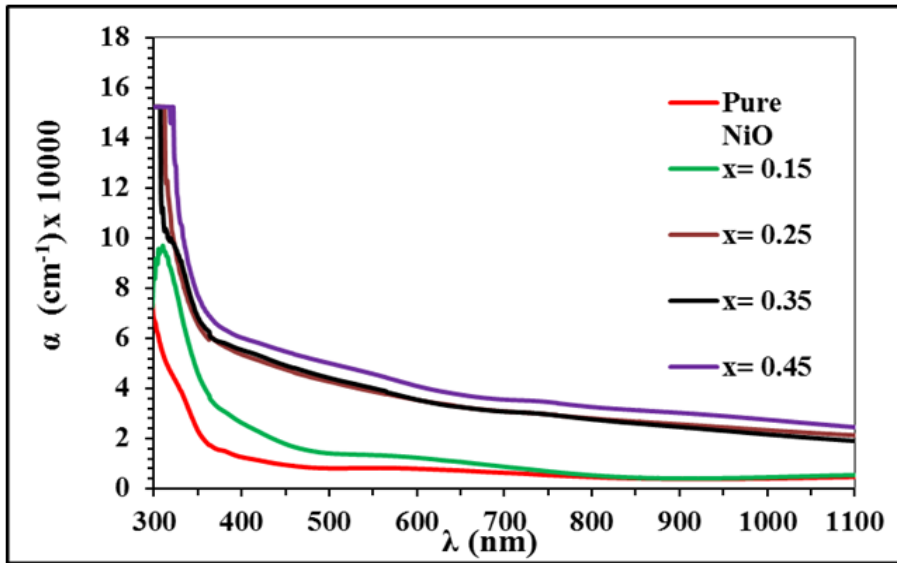


Figure 5. Absorption coefficient for  $(Li_xNi_{2-x}O_2)$  thin films with various values of  $x$  at  $350^\circ C$

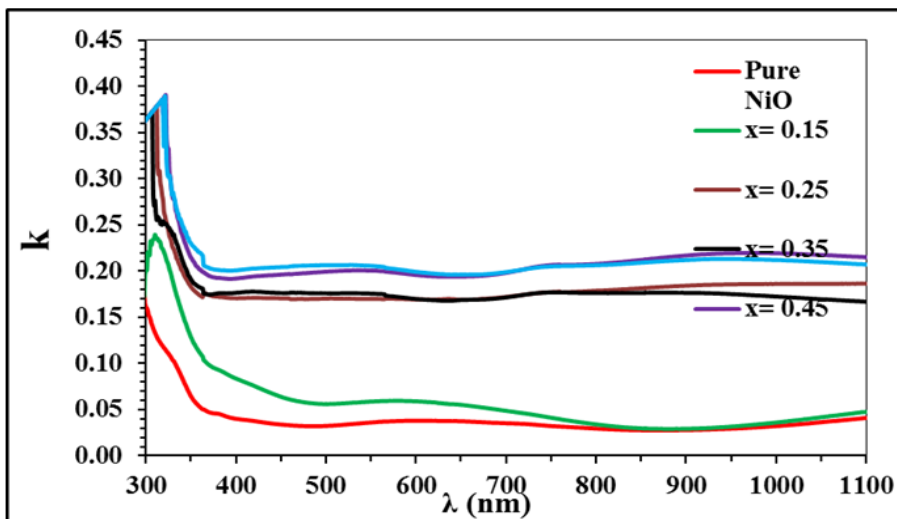


Figure 6. Extinction Coefficient for  $(Li_xNi_{2-x}O_2)$  thin films with various values of  $x$  at  $350^\circ C$

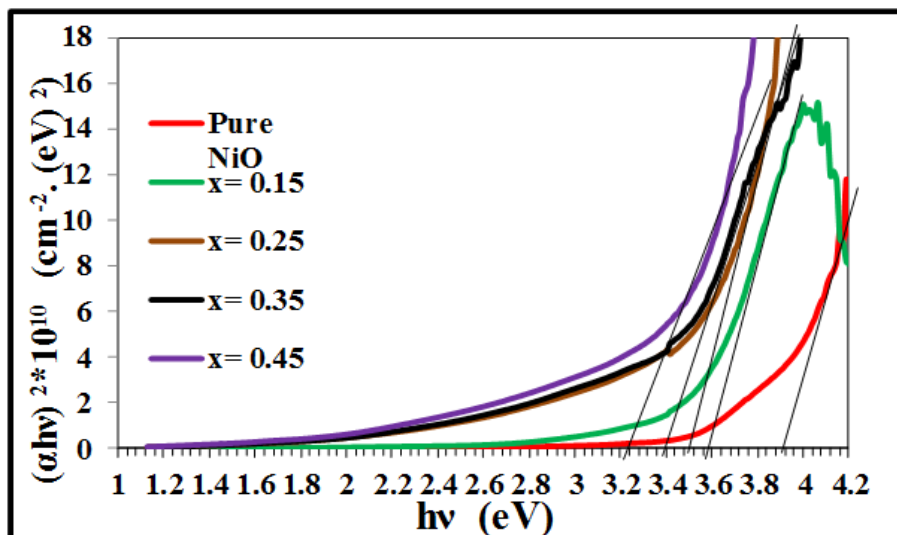


Figure 7. Energy gap for  $(Li_xNi_{2-x}O_2)$  thin films with various values of  $x$  at  $350^\circ C$

### d-Extinction Coefficient (K)

Extinction coefficient of ( $\text{Li}_x\text{Ni}_{2-x}\text{O}_2$ ) films prepared to  $350^\circ\text{C}$  were studied as a function of wavelength. Figure 6 shows that the Extinction coefficient curves is similar to the curves of absorption coefficient. It noticed from Charts and Table 3 notes that the Extinction coefficient decreases with increasing of wavelength, where we note the sharp decline of the coefficient of winding down for all films prepared in the range of wavelengths (300-370nm). generally, Extinction coefficient increase with the increasing of doping for all films which can be explained that the doping with the lithium oxide led to the existence of viable levels near the conduction band led to increased absorption coefficient and thus increase Extinction coefficient this is consistent with. [19]

### e-Energy gap( $E_g$ )

The energy gap for allowed electronic transitions of ( $\text{Li}_x\text{Ni}_{2-x}\text{O}_2$ ) films prepared with various ratios of doping by PLD and annealed to  $350^\circ\text{C}$  are calculated through drawing charts between ( $\alpha h\nu$ ) and the photon energy ( $h\nu$ ). it can be noticed that the optical energy gap starts decrease gradually with the increase in the value of x in the compound ( $\text{Li}_x\text{Ni}_{2-x}\text{O}_2$ ) as shown in Figure 7 which appear decreasing the energy gap of the composite films from (3.90 to 3.28eV) [15], as in Table 3. Diminishing the value of the direct energy gap for all films with the increasing of x value in  $\text{Li}_x\text{Ni}_{2-x}\text{O}_2$  Attributed to changes in the average particle size and improve the crystal structure of the films that's compatible with the testing of XRD and AFM and the results have been reached by researchers [13,14] in the preparation of NiO films with different preparation techniques.

## 4. Conclusions

1- XRD tests for ( $\text{Li}_x\text{Ni}_{2-x}\text{O}_2$ ) films annealed to ( $350^\circ\text{C}$ ) Showed polycrystalline structure with hexagonal installation but pure (NiO) annealed to ( $350^\circ\text{C}$ ) appeared polycrystalline structure with face center cubic.

2- Lithium oxide doping impact on the nature of the crystal structure of a substance nickel oxide multi-gelling and moved from cubic installation to hexagon installation.

3- Particle size values recorded from XRD and AFM measurement for ( $\text{Li}_x\text{Ni}_{2-x}\text{O}_2$ ) films show that grained structures within structures of nanoparticles and doping led to increase particle size.

4- The doping led to decrease in the value of the energy gap for all films.

5- The greatest stable permeability of thin films for the pure (NiO) membrane in the near infrared region and decreased permeability with increase doping.

## References

- [1] D. Franta, Beatrice Negule scu, Luc Thomas, Pierre Richar and Marcel Guyot, "Optical properties of NiO thin films prepared by pulsed Laser deposition technique" Applied surface science, Vol. 244-426, (2005).
- [2] P. Puspaharajah, S. Radhakrishna, A.K. Arof, J. Mater. Sci. 32, 3001, (1997).
- [3] Jiao, Z. M. Wu, Z. Qin, and H. Xu, Nanotechnology 14-458, (2012).
- [4] Souza Cruz, T.G. and M.U. Hleinke, A. Gorenstein, Applied Physics Letters 8-14922, (2002).
- [5] M. Lee, S. Seo, D. Seo, E. Jeong, and I.K. Yoo, Integrated Ferroelectrics 68-19, (2012).
- [6] Zbronic, L. T. Sasaki, N. Koshizaki, Journal of Ceramic Processing Research 6-134, (2005).
- [7] Stamataki, M. D. Tsamakis, N. Brilis, I. Fasaki, A. Giannoudakos, and M. Kompitsas, Physica Status Solidi A-Applied Research 205, 2064-20, (2008).
- [8] M. Rubin, S-J. Wen, T. Richardson, J. Kerr, K. von Rottkay, J. Slack" Electrochromic Lithium Nickel Oxide by Pulsed Laser Deposition and Sputtering" Lawrence Berkeley National Laboratory, University of California (1996).
- [9] G.G. Amatuucci, J.M. Tarascon, D. Larcher, L.C. Klein, Solid State Ionics 84-169, (1996).
- [10] S. Abdelazeem Hassan Abass "Van der Pauw Measurements Of The Hall Effect In Nanoparticulate Silicon Layers" Diploma at AIMS, University of Cape Town, South Africa, (2003).
- [11] Chiwei Wang, Xiaoling Ma, Zicheng Li, Yongguang Liang, Jutang Sun, Yunhong Zhou. "Simple, rapid and accurate determination of lattice composition and evaluation of electrochemical properties of  $\text{Li}_x\text{Ni}_{2-x}\text{O}_2$  electrode material for lithium ion battery by a novel method, Electrochemistry Communications 8, 289-292, (2006).
- [12] Omar Fadhil Abdullah. "Study of physical properties for nano-magnets prepared by mechanical alloying method" college of education, Ph.D. thesis, University of Tikrit, (2016).
- [13] F. Michalak, K. von Rottkay, T. Richardson, J. Slack, M. Rubin. "Electrochromic Lithium Nickel Oxide Thin Films by RF-Sputtering from a  $\text{LiNiO}_2$  Target" Lawrence Berkeley National Laboratory University of California (1998).
- [14] V. Bianchi, D. Caurant, N. Ba ffer, C. Belhomme, E. Chappel, G. Chouteau, S. Bach, J.P. Pereira-Ramos, A. Sulpice, P. Wilmann. "Synthesis, structural characterization and magnetic properties of quasisoichiometric  $\text{LiNiO}_2$ " Solid State Ionics 140, 1-17, (2001).
- [15] H. L. Chen, Y. M. Lu, and W. S. Hwang. "Characterization of sputtered NiO thin film Science ailm", Surface & Coatings Technology, vol. 198, pp. 138-142, (2005).
- [16] M.Z. Obida, H.H. Afify, M.O. Abou-Helal, and H.A.H. Zaid. "Nanocrystalline Anatase Titania Thin Films Synthesized by Spray Pyrolysis for Gas Detection" Egypt. J. Solids, Vol. (28), No. (1) pp.35-51, (2005).
- [17] H.S. Bahidh. "Optical and structural properties of ( $\text{ZnO-SnO}_2$ ) and their Mixture prepared by Chmical Spray Pyrolysis" M.Sc. Thesis, Colleg of Science of women, University of Baghdad, (2009).
- [18] D. Lin-Vien, "The Handbook of Infrared and Raman Characteristic Frequencies of Organic Molecules," Elsevier, (1991).
- [19] Rasheed. Hashim. Jabbar. "Preparation and study of Structural Properties of ZnO, ZnO: Ag Thin Films Prepared by Chemical Spray pyrolysis method and study of Optical Properties before and after annealing", M, Sc. Thesis, college of Education Al-Mustansiriyah University, (2008).